Meteorological Processes Affecting the Transport of Emissions from the Navajo Generating Station to Grand Canyon National Park

CHARLES G. LINDSEY,* JUN CHEN,+ TIMOTHY S. DYE, L. WILLARD RICHARDS, AND DONALD L. BLUMENTHAL

Sonoma Technology, Inc., Santa Rosa, California

(Manuscript received 27 December 1997, in final form 14 October 1998)

ABSTRACT

During the 1990 Navajo Generating Station (NGS) Winter Visibility Study, a network of surface and upper-air meteorological measurement systems was operated in and around Grand Canyon National Park to investigate atmospheric processes in complex terrain that affected the transport of emissions from the nearby NGS. This network included 15 surface monitoring stations, eight balloon sounding stations (equipped with a mix of rawinsonde, tethersonde, and Airsonde sounding systems), three Doppler radar wind profilers, and four Doppler sodars. Measurements were made from 10 January through 31 March 1990. Data from this network were used to prepare objectively analyzed wind fields, trajectories, and streak lines to represent transport of emissions from the NGS, and to prepare isentropic analyses of the data. The results of these meteorological analyses were merged in the form of a computer animation that depicted the streak line analyses along with measurements of perfluorocarbon tracer, SO_2, and sulfate aerosol concentrations, as well as visibility measurements collected by an extensive surface monitoring network. These analyses revealed that synoptic-scale circulations associated with the passage of low pressure systems followed by the formation of high pressure ridges accompanied the majority of cases when NGS emittants appeared to be transported to the Grand Canyon. The authors' results also revealed terrain influences on transport within the topography of the study area, especially mesoscale flows inside the Lake Powell basin and along the plain above the Marble Canyon.

1. Introduction

During the winter of 1990, the Salt River Project (SRP) sponsored the Navajo Generating Station (NGS) Winter Visibility Study (WVS), a large-scale meteorological and air-quality field study conducted in northern Arizona and southern Utah from 10 January through 31 March 1990. The purpose of the WVS was to assess visibility impairment in the Grand Canyon during winter months and to determine the levels of improvement in visibility if sulfur dioxide (SO_2) emissions from the nearby NGS were reduced. Two general approaches were used to meet these goals: 1) the use of data analysis techniques to examine the complex relationships among meteorology, air quality, and visibility during both episode (i.e., periods of poor visibility) and nonepisode conditions; and 2) the use of a deterministic model to simulate the contribution of the NGS and other SO_2 sources to sulfate levels throughout the study area and during episodes when visibility was reduced at the Grand Canyon. Richards et al. (1991) present a complete overview of the study and describe the result of the modeling and analysis efforts. The purpose of this paper is to discuss the meteorological measurements that were made as part of the WVS and to present results of some of the analyses of the meteorological data that were used to characterize transport processes in the Grand Canyon region.

a. Study background

The NGS is located at Page, Arizona, near the Colorado River and Glen Canyon Dam. It consists of three coal-fired 750 MW generating units with emittants vented to the atmosphere through individual 236 m tall stacks. The WVS evolved from an earlier visibility study conducted on the Colorado Plateau in the winter of 1987 referred to as the Winter Haze Intensive Tracer Experiment (WHITEX) (Malm et al. 1989). The purpose of WHITEX was to evaluate the feasibility of alternate approaches for apportioning visibility impairment to a major source. Deuterated methane was released from the NGS stacks as a marker of the plant's emissions.

* Current affiliation: NorthWest Research Associates, Inc., Bellevue, Washington.

+ Current affiliation: Bay Area Air Quality Management District, San Francisco, California.

Corresponding author address: Mr. Charles G. Lindsey, NorthWest Research Associates, Inc., P.O. Box 3027, Bellevue, WA 98009.
E-mail: lin@nwra.com

Ambient concentrations of both the tracer and visibility-related air pollutants were measured in the area of Canyonlands National Park and at other locations, including Hopi Point in the Grand Canyon National Park (GCNP).

As discussed in Richards et al. (1991), the National Park Service (NPS) analyzed the WHITEX data and concluded that the NGS was responsible for a significant portion of the anthropogenic visibility impairment occurring at Hopi Point in the wintertime (Hopi Point, located on the South Rim of the Grand Canyon, was a key receptor site used for data collection during both WHITEX and the NGS WVS). However, considerable controversy surrounded the ability of the WHITEX findings to attribute visibility reduction in the GCNP to NGS emissions (National Research Council 1990), and the SRP undertook the WVS to investigate the problem in more detail. The principal objective of the study was to estimate the level of improvement in visibility in the Grand Canyon during winter that could be attained if NGS emissions were reduced. The NPS and Environmental Protection Agency (EPA) concluded that the primary concern regarding the NGS involved the plant's contribution to visibility impairment due to sulfate formed from its emittants. Therefore, the study focused on the contribution of the NGS to light extinction by sulfates.

b. Overview of the study

For the purposes of both the data analysis and modeling components of the study, three-dimensional pollutant and meteorological measurements were made throughout the study region. Four perfluorocarbon tracer species were released from the NGS to provide a marker that was specific to NGS emittants throughout the study area. The tracers were released one at a time and were changed daily at 1800 MST over a 4-day cycle. Tracer measurements were made at 27 sites to quantify plume dispersion and sample age and to indicate the presence or absence of NGS-specific emittants. The SO_2 and aerosol mass and fine sulfur measurements were made at 26 of these sites. The tracer and SO_2 data were collected in integrated 4-h samples. Visibility measurements were made at Hopi Point and elsewhere in GCNP using integrated nephelometers, which measured light scattering by particles (b_{sp}). In-plume and regional chemical measurements were made by instrumented aircraft to quantify the parameters needed for modeling and analysis purposes. Measurements were made at the boundaries of the region to quantify the pollutants transported into the study region from upwind sources. Data for sulfur-size distributions and for other species were obtained at key receptor sites and elsewhere to assess the relative contribution of sulfate to visibility impairment at GCNP. Richards et al. (1991) discuss in detail the scope of these measurements made during the field study.

An important component of the study was the operation of a network of meteorological monitoring stations that routinely collected surface and upper-air data. A network of 15 surface stations measured winds, temperatures, moisture, and in some cases solar radiation and precipitation. Upper-air wind and thermodynamic data were collected at 12 sites in the study area using several different measurement techniques, including rawinsonde sounding systems, Doppler sodars, Doppler radar wind profilers, Airsondes, and tethersondes. The majority of this network operated continuously during the study. During intensive operational periods (IOPs), which were called based on meteorological and pollutant forecasts, upper-air data collection was enhanced at some of the sites by the collection of additional rawinsonde and tethersonde soundings. IOPs were called for days when forecasted conditions indicated that high levels of regional haze were expected [e.g., $b_{sp} \geq 10$ inverse megameters (Mm^{-1}) at Hopi Point], when the NGS plume interacted with clouds or experienced conditions of high relative humidity, and/or when plume-height winds were expected to be from 300° to 75° true, which might transport NGS emissions toward GCNP. During IOPs the instrumented aircraft flew and supplemental surface air-quality data were collected.

The design of the monitoring network was based on collecting data that would resolve processes on the principal scales of motion that were expected to be responsible for transporting emittants from NGS, given the complex topography of the study area. For example, under some circumstances, it was expected that NGS emittants would be carried to the Grand Canyon by winds driven principally by the synoptic-scale pressure gradient, which could be resolved by a few, carefully placed measurement stations (e.g., northeasterly winds accompanying passage of a low pressure system or development of a ridge of high pressure). However, it was also anticipated that topographical influences would cause the winds within the lower parts of the atmospheric boundary layer (ABL) or at plume-carrying altitudes to become decoupled from the synoptic-scale flows at higher altitudes, owing to the development of terrain-induced circulations. Under such conditions, a more dense network of observations would be needed to examine transport mechanisms.

The purpose of this paper is to describe the meteorological measurement component of the Navajo Generating Station Winter Visibility Study and to report on the results of some of the transport analyses that were performed to determine periods when NGS emittants might have reached the Grand Canyon. A series of companion papers describe the structure of the boundary layer inside the Grand Canyon itself (Whiteman et al. 1998a); three-dimensional airflows within and above the canyon based on Doppler lidar measurements taken from the South Rim of the Grand Canyon (Banta et al. 1999); surface and aloft wind flow patterns across the study area (Allwine et al. 1998, manuscript submitted to *J. Appl. Meteor.*; Whiteman et al. 1999b); and a case study of long-range transport to the Grand Canyon

(Chen et al. 1999). In addition to the analyses described in this series of papers, other analyses were conducted by study investigators that will not be described in detail here but that represented important components of the study. These analyses included determining the contribution of NGS emissions to sulfate concentrations in GCNP, characterizing the effects of sulfate concentrations on visibility, and evaluating the representativeness of the 1990 study period relative to that of other years. Richards et al. (1991) describe these analyses in detail.

2. Overview of the meteorological measurements

Many authors have described meteorological processes in complex terrain and how they affect the evolution of the daytime convective boundary layer (CBL), the nighttime nocturnal boundary layer, and ultimately the dispersion of pollutants emitted into the lower atmosphere in such environments (e.g., Orgill 1981; Atkinson 1981; Whiteman 1990). Some of these processes include thermally driven slope and valley wind systems, topographic channeling of flows, formation and destruction of basin and valley inversions, and fumigation of aloft plumes by the growing CBL. The philosophy behind the design of the meteorological network deployed for the NGS Winter Visibility Study was to select and position measurement systems so that the cumulative affect of these processes could be monitored along the major topographic channels in the region. The next sections briefly describe the topography of the study area and the design of the meteorological measurements network.

a. Topography of the study region

The NGS is located in what is referred to as the Colorado Plateaus Province in the western United States. This province constitutes a large drainage basin in western Colorado, northwestern New Mexico, eastern Utah, and northern Arizona. The principal rivers draining the province are the Colorado, Green, San Juan, and Little Colorado. The Colorado River leaves Colorado near Grand Junction and meets the Green River near Canyonlands National Park southwest of Moab, Utah. Not far from this junction the Colorado River enters Lake Powell. The Glen Canyon Dam at Page, Arizona, backs up the Colorado River to form Lake Powell. The San Juan River enters Lake Powell west of Mexican Hat, Utah. From Lake Powell, the Colorado River flows southward through the Marble Canyon toward the Grand Canyon. On the eastern edge of Grand Canyon National Park, the river is joined by the Little Colorado River. The Colorado River then turns westward to flow through the Grand Canyon. On the western end of the Grand Canyon is Lake Mead, an artificial reservoir created by the Hoover Dam.

The major topographic features of the study area are shown in Fig. 1. Key features in the region include the elevated Kaiparowits Plateau that, with its extensions to the southeast toward Black Mesa, forms a topographic block to the Colorado River airshed north of the NGS. An area of high plateaus, including the Aquarius and Markagunt plateaus, is located northwest of Page. The Kaibab Plateau southwest of Page, and to a lesser extent the Paria Plateau west-southwest of Page, constitute the remainder of the nearby elevated terrain. The western boundary of the Colorado Plateaus Province runs north–south to the west of Page. A low pass in the boundary occurs between Page and Fredonia. The next main break in the boundary is the Grand Canyon itself, a deep narrow canyon cut between the Kaibab Plateau and the elevated plateaus farther south.

Before reaching the Grand Canyon, the Colorado River cuts through the Marble Canyon plain. The plain into which the Marble Canyon has been eroded is tilted downward toward the north-northeast, counter to the direction of flow of the Colorado River. The depth of the canyon thus increases rapidly from zero width and depth at the northern edge of the plain to 3.5 km wide and 720 m deep just east of one of the measurement sites located on the plain at Buffalo Ranch (see next section). Once the river turns westward, it cuts deeply through the middle of an elevated mass of uplifted strata that attains heights of nearly 2300 m on the South Rim and 2844 m on the North Rim. The North Rim is the southern edge of the Kaibab Plateau, which in winter has a permanent snow cover. At the bottom of the canyon below the South Rim is Phantom Ranch, a camping facility run by the NPS. As discussed in the next section, Phantom Ranch was used to collect surface and upper-air data inside the canyon. Whiteman et al. (1998a) describe the structure of the boundary layer inside the Grand Canyon based on analyses of these data.

b. Description of the measurement network

Figure 2 shows the locations of the surface and upper-air stations deployed for the NGS Winter Visibility Study [Winslow is actually a National Weather Service (NWS) surface and rawinsonde sounding station]. Table 1 lists the locations and altitudes of these stations. The formal period of operation of this network was from 10 January 1990 through 31 March 1990. However, some stations began collecting data before January 10 and a few measurements were discontinued after 19 March 1990. Lindsey et al. (1991) describe the periods of data collection in more detail.

Data collected at the surface stations included hourly averaged measurements of winds, temperature, and moisture. Several stations also measured precipitation and direct and reflected solar radiation. Hauser et al. (1991) discuss the operation of the surface network in more detail. Rawinsonde soundings were collected twice daily (0400 and 1600 MST) at Bullfrog Basin (BUL), Tusayan (TUS), and Ash Fork (ASH) on every day of the study and four times daily (0400, 1000, 1600,

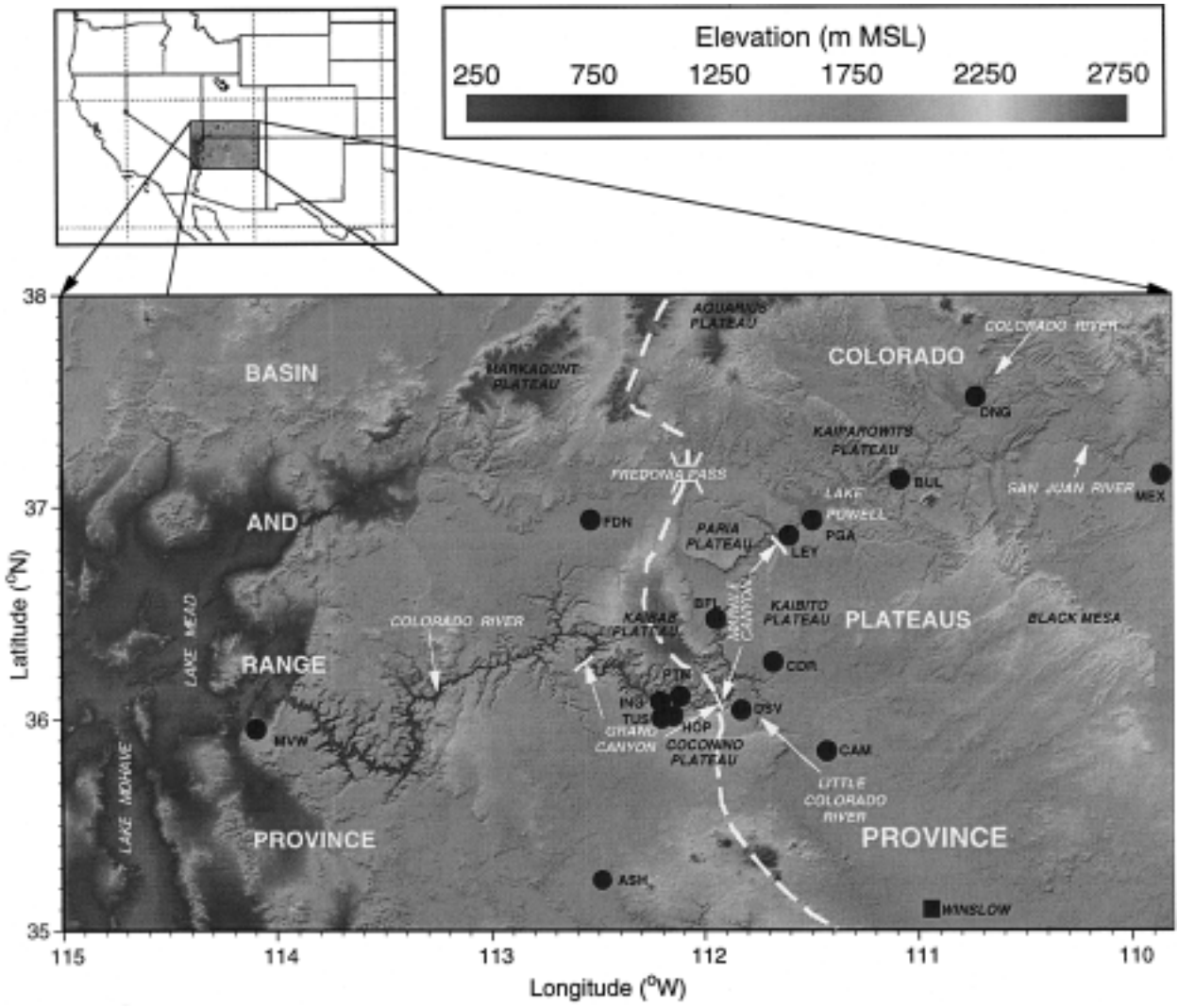

FIG. 1. Topography of the NGS Winter Visibility Study region.

and 2200 MST) during IOPs at BUL, Dangling Rope (DNG), Cameron (CAM), and TUS. Data in these soundings included vertical profiles of winds, temperature, pressure, and moisture as a function of altitude. Thermodynamic data (pressure, temperature, moisture only) were collected twice daily (0400 and 1600 MST) at Cedar Ridge (CDR) using an Airsonde sounding system. An optically tracked Airsonde system was also used to collect upper-air winds and temperatures at Page (PGA) twice daily each day of the study and four times daily during IOP periods at the same sounding times mentioned previously. Airsonde soundings were also taken from Phantom Ranch (PTN) at the bottom of the Grand Canyon during IOP periods. During IOPs, tethersonde profiles were collected at Phantom Ranch and at Buffalo Ranch (Whiteman et al. 1991).

A network of three 915-MHz Doppler radar wind profilers measured upper-air winds on a daily basis during the study (Lindsey and Wolfe 1991). These data were reported as hourly averages, with a vertical resolution of approximately 100 m over a range of 1–4 km above ground level (the maximum altitude to which the profilers could sample varied depending on atmospheric conditions). One profiler was located at Page, the second at Cedar Ridge, and the third inside the Grand Canyon itself at Phantom Ranch. A network of four Doppler sodar systems collected hourly averaged profiles of winds aloft on a daily basis at four sites: Mexican Hat (MEX), Fredonia (FDN), Dangling Rope, and Cameron. The sodars sampled winds aloft from 30 m above ground level (AGL) to approximately 750 m AGL, with a vertical resolution of 30 m. A high-resolution, facsimile sodar was also operated at Page to map boundary layer heights and gravity wave structures. In addition, a Doppler lidar positioned near Desert View (DSV) was used to investigate flows in the Grand Canyon itself

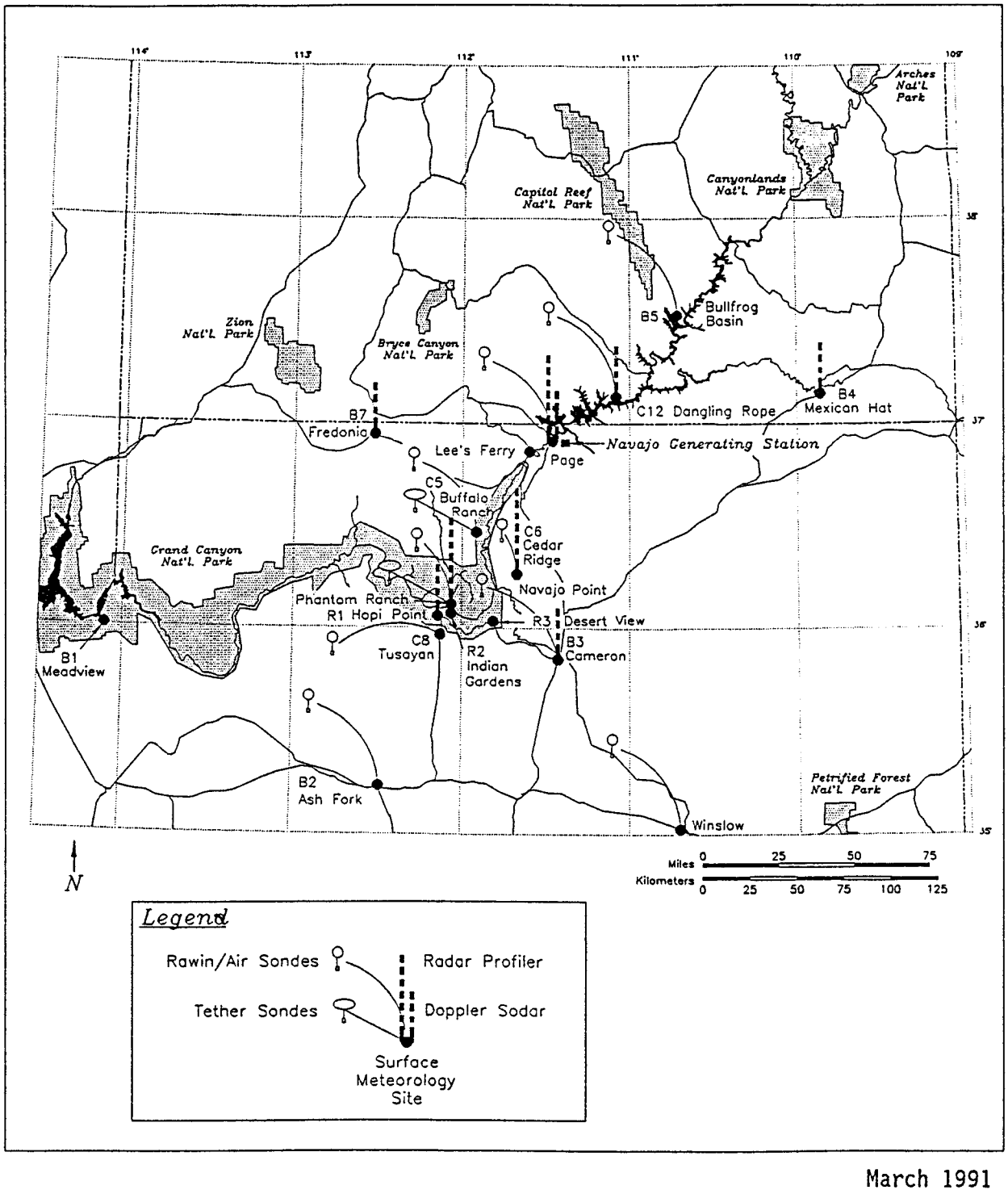

FIG. 2. Map of the study region and locations where surface and upper-air meteorological data were collected.

(Banta and Olivier 1991). Finally, a variety of NWS data and products were archived during the study period to help with analysis and interpretation of the WVS data (e.g., hourly surface observations, upper-air data, surface and constant level charts, satellite imagery, etc.).

3. Transport analysis techniques

Analyses of the transport of NGS emittants were performed using a number of analytical techniques, which included, among others, the following.

TABLE 1. Sites where meteorological data were collected during the 1990 NGS Winter Visibility Study. *X* and *Y* are the grid coordinates of the stations in the wind field model domain (see text for explanation).

Site name	Site ID	Obs	Lat	Long	Alt (m MSL)	UTM E (km)	UTM N (km)
Bullfrog Basin	BUL	S, R	37°31′08″	110°43′30″	1130	524.3	4152.4
Dangling Rope	DNG	S, R, DS	37°07′48″	111°04′53″	115	492.7	4109.2
Cameron	CAM	S, R, DS	35°50′54″	111°25′39″	1350	461.3	3967.2
Tusayan	TUS	R	38°58′05″	112°07′35″	2012	398.4	3980.9
Ash Fork	ASH	S, R	35°14′21″	112°29′00″	1588	365.0	3900.5
Cedar Ridge	CDR	S, P, A	36°15′55″	111°40′35″	1786	439.2	4013.5
Mexican Hat	MEX	S, DS	37°08′56″	109°51′42″	1271	601.2	4111.8
Fredonia	FDN	S, DS	36°56′17″	112°31′46″	1420	364.0	4089.6
Lee's Ferry	LEY	S	36°51′48″	111°36′00″	994	447.5	4081.0
Hopi Point	HOP	S	36°04′16″	112°09′14″	2152	396.5	3990.8
Indian Gardens	ING	S	36°04′45″	112°07′37″	1146	404.1	3992.3
Desert View	DSV	S, L	36°02′29″	111°49′39″	2283	425.5	3989.0
Meadview	MVW	S	35°57′12″	114°05′46″	1070	220.3	3988.8
Buffalo Ranch	BFL	S, T, A	36°28′11″	111°56′43″	1710	413.8	4034.4
Phantom Ranch	PTN	S, P, T, A	40°00′00″	105°00′00″	750	404.6	3997.2
Page	PGA	S, P, A	36°54′00″	111°30′00″	1322	458.4	4085.3

Key to observations: S—surface; R—rawinsonde; A—airsonde; T—tethersonde; DS—Doppler sodar; P—radar wind profiler; and L—Doppler lidar.

- Wind field and trajectory analyses were prepared for each day of the 81-day study to examine transport of air parcels passing over Page at selected altitudes.
- A computer animation was developed to show air parcel streak lines at several altitudes encompassing likely plume heights (to represent the ''centerline'' of the NGS plume). The animation also depicted network-wide surface PFT tracer observations and surface SO_2 and sulfate aerosol concentrations, as well as b_{sp}, relative humidity, and precipitation at Hopi Point, for each sample period during the 81-day study. This animation was used to assist researchers in locating NGS emittants in the study region.
- Isentropic analyses were performed to examine wind and stability relationships responsible for plume transport and mixing along an axis connecting the Lake Powell basin, the Marble Canyon plain, and the Grand Canyon.
- A number of graphical data products were generated, including time–height cross sections of winds aloft at each of the upper-air stations; time–height plots of the rawinsonde data, which included displays of the altitudes of the 700-mb and 500-mb pressure surfaces; and time series plots of surface data.

The computer animation was an important tool for locating NGS emittants and analyzing transport mechanisms in that it allowed the meteorological, tracer, SO_2, and related data to be integrated into a time varying, three-dimensional representation of the conditions encountered during the field study. The isentropic and other analyses and data products were useful for studying specific conditions, especially when complex circulations formed. The following sections briefly describe how these analyses were prepared, and then summarize the results obtained using these techniques.

a. Wind field and trajectory analyses and preparation of computer animation

Because of the duration of the field study and large volume of data collected, relatively simple techniques were needed to estimate locations of NGS emittants from the meteorological data for display in the computer animation. These simple techniques were justified in part because the tracer and SO_2 data, which were collected at a number of sites in the study area as well as at the Grand Canyon itself, also would provide indications of the location of NGS emittants. The other analytical tools also would assist in resolving conditions that might be poorly represented in the animation. The technique chosen to analyze the meteorological data for the animation was to calculate objectively analyzed, mass consistent wind fields for each hour of the study period from l0 January 1990 through 31 March 1990, using a pair of kinematic wind field models developed at the California Institute of Technology by Goodin et al. (1980) and later modified by the California Air Resources Board. One model calculated surface wind fields from the hourly data collected by the tower network. The second model calculated aloft wind fields, using the results of the surface model and the winds aloft observations from the upper-air network. The surface model included very simple parameterizations for the effects of atmospheric stability, mixing depth, and topographical forcing to compute surface wind fields. The upper-air model included simple parameterizations for stability effects and mixing depth, principally through filters and averaging schemes applied to the interpolated data. The main function of the upper-air model was to calculate interpolated wind fields at user-specified altitudes and then adjust these wind fields to obtain mass

balance by application of the incompressible form of the continuity equation.

These models are not rigorous in their treatment of physical processes that govern the evolution of flows within the modeling domain. At the same time, they are not as computationally intensive as prognostic models that solve the basic set of equations derived from first principles that describe atmospheric behavior. Rather, the diagnostic models are data interpretation tools whose results will only be as good as the quality and resolution of the original observations collected in the field. For this study, the resolution (space and time) of the upper-air data was comparable to that of the surface data. While the simple parameterizations for stability and terrain effects can and did influence the resulting wind fields, the major influence on the results obtained from these models stemmed from how well circulations within the topography of the study region were represented in the data collected at the surface and upper-air sites.

Data used in the wind field computations included the hourly averaged surface winds from the tower network and winds aloft measured by the Doppler radar profilers (hourly averages), Doppler sodars (hourly averages), and rawinsonde sounding stations. Only data that had received level 1 quality-control screening (Lindsey et al. 1995) were used in the wind field computations. Missing data were interpolated linearly in time in both the surface and upper-air models; a cubic polynomial was used to interpolate missing data in the vertical in the upper-air model. The wind fields were prepared over a domain that was 500 km (east–west) by 400 km (north–south), roughly centered on Page and comparable to the area shown in Fig. 2. A horizontal grid of 100 $\times$ 80 grid points was defined over this area with horizontal spacing of 5000 m in both the north–south and east–west directions. A terrain data file was prepared for this grid for use in the surface wind field model, using a USGS digital topography database. Ten vertical levels were specified in the upper-air model: 10 m, 150 m, 300 m, 450 m, 600 m, 750 m, 900 m, 1200 m, 1500 m, and 2000 m (all heights above ground level). The data at 10 m AGL were supplied by the output from the surface model. The upper-air model used a terrain following coordinate system, so that the wind fields were computed on AGL surfaces.

From the wind field analyses, forward trajectories of air parcels starting each hour above Page were calculated to simulate the transport of emittants from NGS at plume carrying altitudes. Trajectories were calculated for 300 m, 600 m, and 750 m AGL. These altitudes were chosen to represent average plume rises from NGS and to examine the coupling and decoupling of flows in the lower boundary layer from flows at higher altitudes. These altitudes also represented the range of elevations with the greatest rate of recovery for the upper-air data, which was dictated principally by the Doppler sodar systems. From the trajectory analyses, streak lines were prepared to represent the centerline of the plume at each hour of the study from 10 January at 0000 MST to 31 March at 2300 MST. (In the strictest sense, a streak line defines the line at a particular moment in time connecting all air parcels that have passed a given geometric point, in this case 300 m, 600 m, and 750 m AGL above Page.)

To improve computational efficiency in the animation software, the location of the ''plume'' along the streak lines was represented in the computer animation by circles that began every 2 h at Page and whose position along a streak line was updated hourly. The 4-h integrated tracer and SO_2 data collected by the surface chemistry network were also depicted in the animation. Figure 3 shows an example of one frame from the animation. One of four colors was used for the circles to represent the tracer that was being emitted from NGS at the time the circle was ''released.'' Based on the work of Smith (1981), the diameter of each circle was given by

$$\text{diameter} = 2x^{0.8},$$

where x was the cumulative distance traveled from Page. The size of the circles was not designed so much as a representation of horizontal dispersion as it was an analogy for the age of the simulated air parcel. By varying the size of the circles, one could distinguish ''fresh'' air parcels from ''aged'' air parcels in the animation.

The 4-h integrated tracer and SO_2 concentrations were indicated by bar graphs at the surface sampling sites. In the animation, the bars for the tracer concentrations were color coded using the same color for each tracer as was used for the streak lines. Hourly integrated nephelometer readings and hourly averaged relative humidity data from Hopi Point also were shown in the animation. The Hopi Point b_{sp} and relative humidity values were represented in a ''strip chart'' format in the animation. Forty-eight hours of hourly averaged data were presented, with the center of the display (indicated by ''bouncing balls'') synchronized with the animation. The horizontal scale showed the previous and next 24 h of data relative to the current time, with tick marks every 4 h corresponding to the sampling periods for the tracer and SO_2 data. The color of the ''bouncing ball'' for the relative humidity data changed when the Hopi Point surface meteorology station reported that precipitation was falling at Hopi Point.

b. Isentropic analyses

Isentropic analyses were performed to examine wind and stability relationships within the complex topography of the study area. The goal of these analyses was to try to identify periods when the transport of NGS emittants was coupled to synoptic-scale flows versus periods when winds carrying NGS emittants within the topography of the study area had become decoupled from the synoptic-scale forcing and were instead responding principally to terrain-driven processes. Iden-

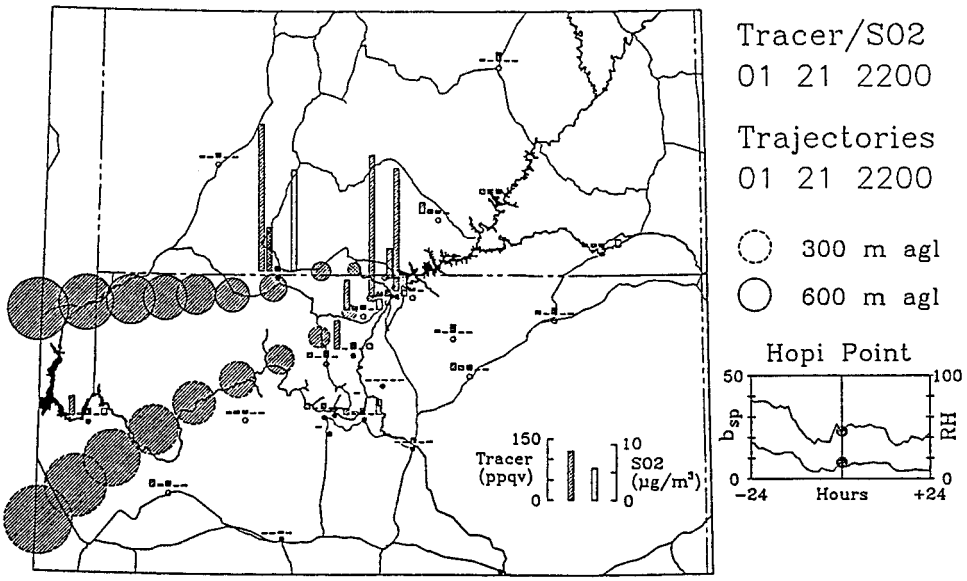

FIG. 3. Example of a single frame of the computer animation, showing the locations of the 300 and 600 m AGL streak lines and Hopi Point b_{sp} and relative humidity at 2200 MST 21 January 1990; tracer and SO_2 concentrations shown were collected from 2200 MST 21 January until 0200 MST 22 January 1990.

tifying periods of coupling and decoupling was important to understanding how well the computer animation was resolving the location of emittants from NGS.

Vertical isentropic cross sections were prepared along the ground path shown in Fig. 4. This path was designed so that upper-air data (rawinsondes, Airsonde, tethersondes) from BUL, DNG, PGA, CDR, PTN, TUS, and ASH could be used, as available, for computation and analysis of levels of constant potential temperature (isentropes) as a function of altitude. Wind data from the radar profilers and rawinsonde stations also were displayed. Isentropic cross sections were prepared for the 0400 and 1600 MST soundings for all study days, and for the 1000 and 2200 MST soundings on IOP days. An example of such a cross section for 20 January 1990 at 1600 MST is presented in Fig. 5. The Briggs plume height estimate of the altitude of the NGS plume is indicated by the star above Page (Briggs 1972).

The results presented in Fig. 5 indicate that a relatively neutral boundary layer had developed over the entire study area by the afternoon of 20 January. Judging from the location of the inversion, this boundary layer was approximately 1200 m deep over the Lake Powell basin and 700 m deep over the high terrain south of the Grand Canyon. The Briggs plume height estimate indicated that the plume from NGS was located at the base of the inversion where northeasterly winds could transport emittants toward the Grand Canyon. These northeasterly winds were coupled to the synoptic-scale flows, which were northeasterly from approximately 2300 m MSL to above 4000 m MSL. However, flows within the Lake Powell basin above Page were easterly, and winds along the Marble Canyon plain at Cedar Ridge were northerly. These results indicate that the flows within the terrain were being affected, perhaps channeled, by the topography of the Lake Powell basin and by the Kaibab Plateau, which runs approximately north–south along the western edge of the Marble Canyon plain. In this example, the winds at plume height are driven by the synoptic-scale forcing, but winds below the tops of the terrain were somewhat decoupled from flows aloft.

4. Results of the transport analyses

The animation and supporting analyses were used to categorize each of the 4-h sample periods as to whether or not emittants from NGS may have been present at the Grand Canyon during the sampling period, based on conditions observed at the Grand Canyon sampling sites located at Hopi Point, Desert View, and Indian Gardens. Table 2 lists the categories that were defined for this analysis. The function of these categories was as follows.

- Categories 1–6 were used to indicate that emittants from NGS were probably present at the Grand Canyon during the 4-h sample, with the distinctions between the categories based on time of arrival or transport pathway.
- The definition of direct transport versus second day versus aged emittants was defined based on emittants reaching a receptor during or after the 0600 MST sample.
- Categories 5 and 6 were used to represent possible low-level transport of emittants, which had mixed into

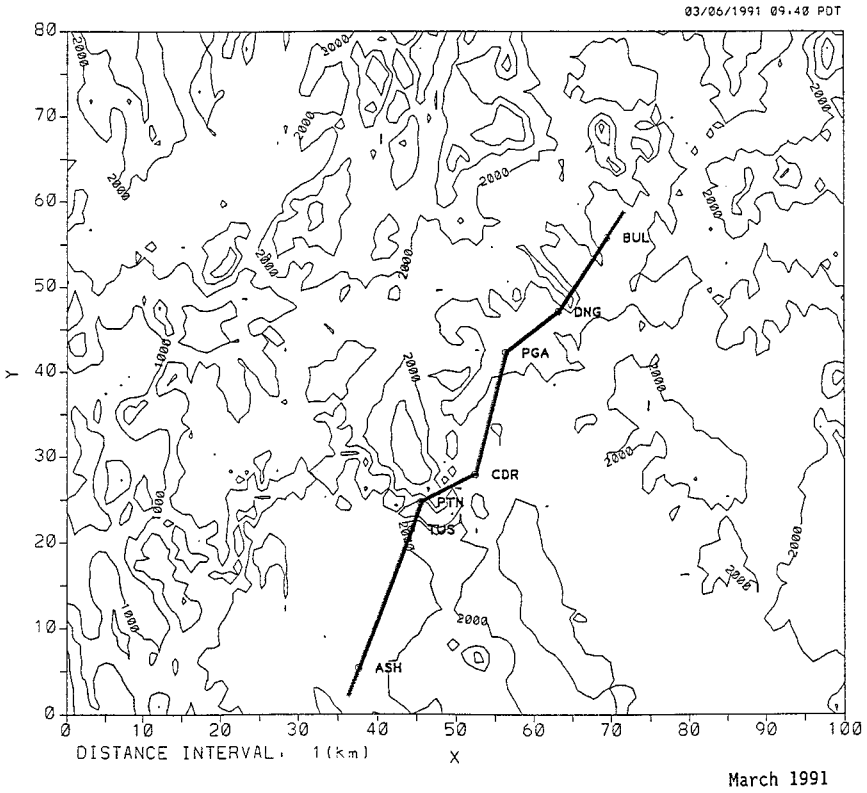

FIG. 4. Ground path between Bullfrog Basin and Ash Fork along which longitudinal isentropic cross sections were prepared; contours indicate terrain elevations (m MSL).

the surface layer under conditions when low-level flows may have been decoupled from flows aloft at plume heights.
- Categories 7 and 8 were not used in the present analyses but left as ''place holders'' for future analyses.
- Category 9 was used to indicate periods that could not be categorized easily from available information and therefore required additional investigation; these periods were subsequently reassigned to one of the other categories as the analyses proceeded.
- Category 10 indicated that emittants from NGS were probably not at the Grand Canyon.

In the course of reviewing the animation and deciding whether or not emittants from NGS were at the Grand Canyon, the isentropic analyses, time–height cross section plots, time series plots, and other supporting data products were reviewed to verify or reject the results evident in the animation. This was particularly useful when the tracer and SO_2 data confirmed that the plume had mixed to the surface, often as a result of fumigation as the CBL grew and intercepted the aloft plume. When emittants appeared at the surface sampling sites in the major drainage basins of the Grand Canyon (e.g., Lake Powell basin, Marble Canyon basin, etc.), the isentropic cross sections and time–height cross sections were studied for evidence of low-level flows that might have carried emittants toward the Grand Canyon.

To represent which combination of the meteorological, tracer, and SO_2 datasets confirmed the presence or absence of emittants at the Grand Canyon, indices were defined based on which of the three datasets were used to assign a particular category to a 4-h sampling period. Each 4-h period was assigned a category, which, in turn, was assigned an index that indicated which of the datasets was used as the basis for selecting the category. Table 3 lists and defines these indices.

Figure 6 shows the number of 4-h periods assigned to each of the categories listed in Table 2. There were 486 4-h sample periods between 10 January and 31 March. Note that 507 categories were assigned to these 486 sample periods. On 21 occasions, it was appropriate to assign more than one category to indicate that emittants were probably present, for example, both direct and second-day emittants were evident at a receptor during the 0600 MST–1000 MST sample. Based on at least one category (1–6) indicating that NGS emittants were probably present, the results presented in Fig. 6 show that emittants from NGS were probably present at the Grand Canyon approximately 33% of the 4-h sample periods. Likewise, emittants were probably absent (category 10) approximately 67% of the 4-h samples. No significant differences were evident between day and night. While it is difficult to absolutely quantify the uncertainties in these estimates, given that the de-

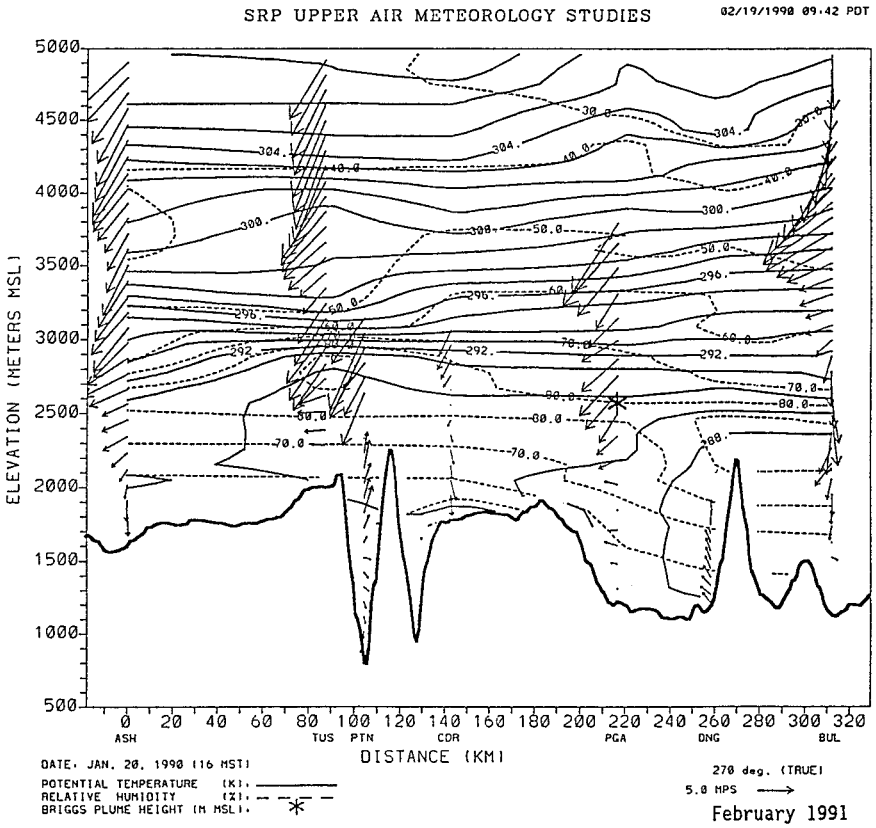

FIG. 5. Isentropic cross section for 1600 MST 20 January 1990. Solid lines are isentropes, dashed lines are isopleths of constant relative humidity, and vectors indicate wind speed and direction (north to top of figure, east to right of figure). The heavy solid line represents terrain elevations along the ground path of the cross section. Briggs plume height estimate of the altitude of the NGS plume is indicated by a star above Page.

TABLE 2. Definition of categories used to classify 4-h sampling periods as to whether or not NGS emittants were present at the Grand Canyon.

Category	Description
1	Direct transport of emittants to receptor. ● Emittants arrive before dawn of the day following the next tracer release.
2	Second-day emittants at receptor. ● Emittants reach receptor after the tracer has been changed once and after dawn of the day following release.
3	Aged emittants at receptor. ● Emittants reach receptor after the tracer has been changed two or more times and after dawn of the second day since release.
4	Emittants at receptor that appear to arrive via transport path that goes off the modeling grid.
5	Possible transport of emittants to a receptor via surface (low level) transport through Marble Canyon.
6	Possible transport of emittants to a receptor via surface (low level) transport from the east.
7, 8	Reserved for future use.
9	Further investigation needed.
10	No emittants at receptor site.

cision-making process to assign the categories contained a subjective element, at least two of the three datasets confirmed 98% of the category assignments when emittants were judged to be probably absent. When emittants were judged to be probably present, 57% of the

TABLE 3. Definition of indices used for specifying which of the streak line, tracer, and SO_2 datasets were used to assign a category to a 4-h sample.

Index	Description
10	Indicated by streak lines, tracer, and SO_2.
20	Indicated by streak lines and tracer, but not by SO_2.
21	SO_2 data not available.
30	Indicated by streak lines and SO_2, but not by tracer.
31	Tracer data not available.
40	Indicated by tracer and SO_2, but not by streak lines.
50	Indicated by streak lines, but not by tracer or SO_2.
51	Tracer data not available.
52	SO_2 data not available.
53	Neither tracer nor SO_2 data available.
60	Indicated by tracer, but not by streak lines or SO_2.
61	SO_2 data not available.
70	Indicated by SO_2, but not by streak lines or tracer.
71	Tracer data not available.

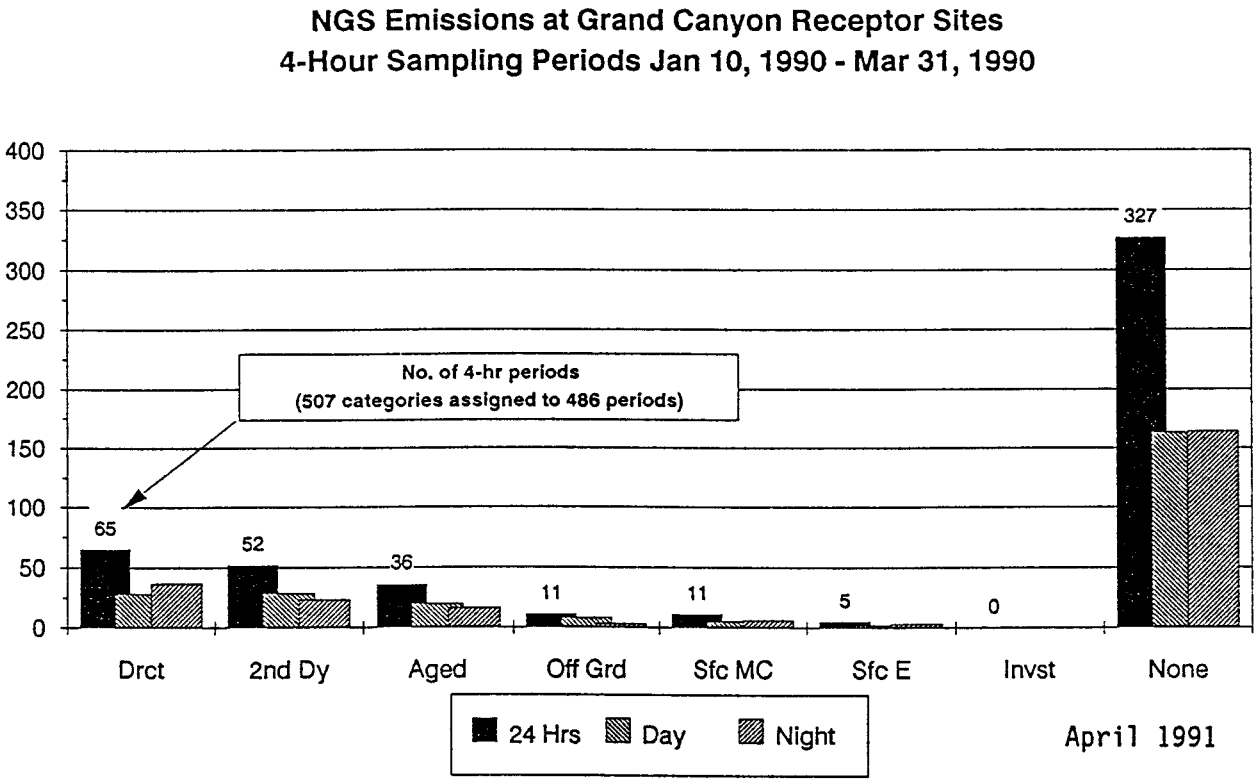

FIG. 6. Distribution of number of categories assigned to indicate the presence or absence of NGS emittants at the Grand Canyon for the period 10 January 1990–31 March 1990.

category assignments were based on two or three of the datasets confirming the category selection. This suggests a relatively high degree of confidence in knowing when emittants were probably absent and a somewhat lower degree of confidence that indeed emittants from NGS were probably present during all the 4-h periods assigned a category value of 1–6.

In addition to indicating those times that NGS emittants were carried toward the Grand Canyon, the animation also showed that the NGS plume was carried to the northeast, up Lake Powell, on a frequent basis under a prevailing southwesterly wind regime. During these periods, the animation showed that NGS emittants were mixed into the Lake Powell basin on a regular basis. High tracer and/or SO_2 concentrations often appeared during the 1000 and 1400 MST sample periods in the animation, indicating fumigation of the NGS plume as the CBL grew during the day.

Whiteman et al. (1991) reported that low-level easterly winds formed in the Lake Powell basin under clear sky, light wind conditions. However, these flows did not exhibit a diurnal variation, indicating they were not thermally forced by the heating and cooling of the surrounding terrain. Rather, they were correlated with synoptic-scale pressure gradients across the desert Southwest. These easterly flows appeared to be compensation currents that were channeled through the low-lying passes in the study area and through the Grand Canyon itself. The possibility of these flows carrying emittants out of the Lake Powell basin toward GCNP, especially during stable, decoupled conditions, was investigated. Once emittants were in the Lake Powell basin, the animation was carefully reviewed for the possibility of emittants being transported out of the basin toward the Marble Canyon and the Grand Canyon. On a few occasions, the tracer and SO_2 data indicated that indeed this process may have occurred even while the main transport aloft was in a different direction, but the isentropic analyses, time–height cross sections of winds aloft at Page and Cedar Ridge and the time series plots of surface winds did not indicate that this was an important mechanism for transporting NGS emittants to the Grand Canyon.

Figures 7 and 8 are isopleths of the locations of the 300 and 600 m AGL streak lines presented in the animation. The isopleths represent the number of times that a streak line was closest to (or passed over) a grid point in the modeling domain (for reference, there were 972 streak lines used in these analyses: 12 per day for 81 days). Visual inspection of the animation indicated that the 600 m AGL streak line passed over the Grand Canyon approximately 17 times during the field study, in general agreement with the results presented in Fig. 8. The results presented in these two figures indicate that

- The preferred transport direction for NGS emittants

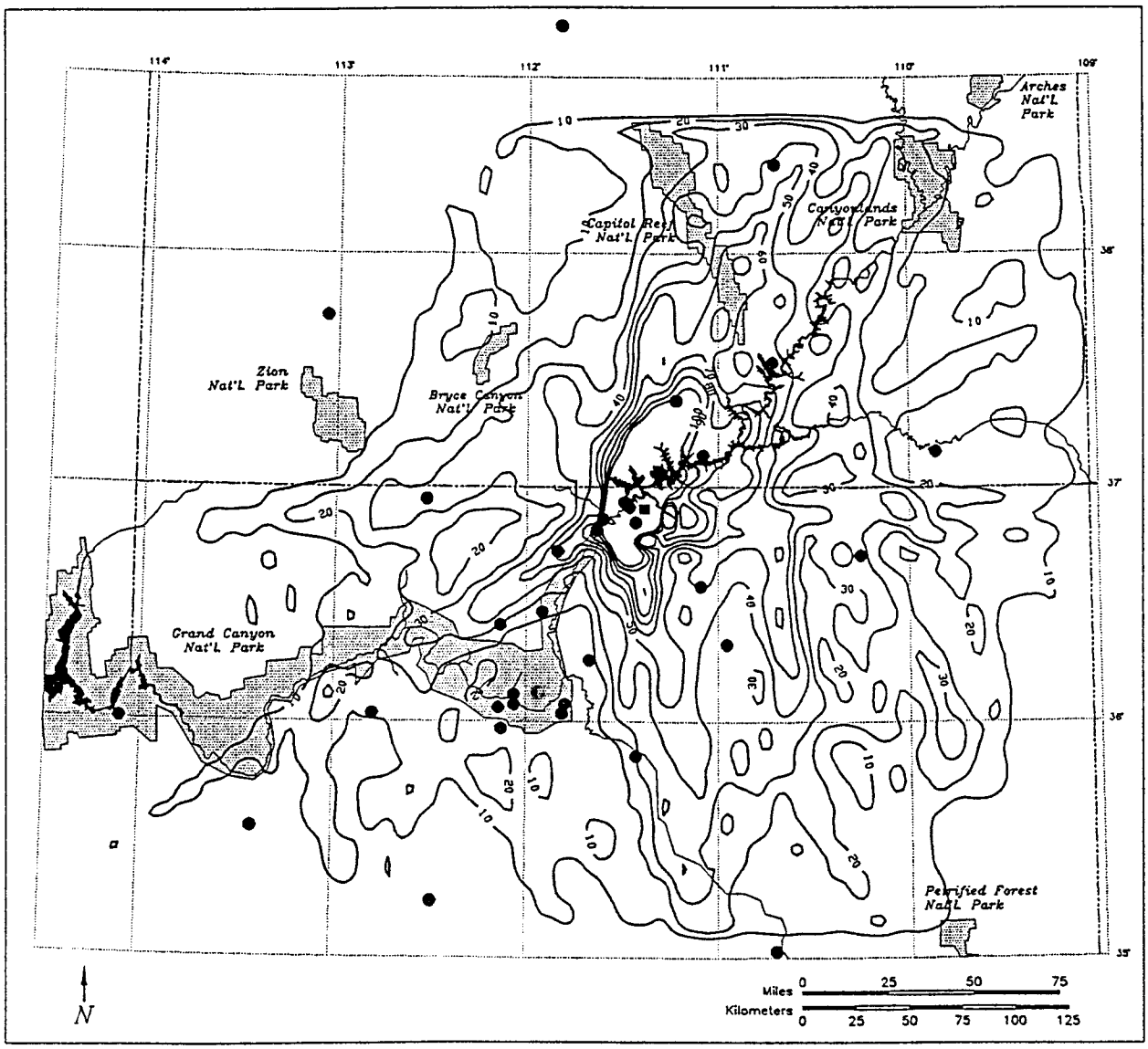

FIG. 7. Isopleths of the number of times a streak line at 300 m AGL passed a grid point in the modeling domain of the wind field and trajectory models for the period 10 January 1990–31 March 1990.

was to the northeast up Lake Powell during the study period, driven by prevailing southwesterly winds;
- Transport to the west from Page toward the Fredonia Pass is evident in the 300 m AGL streak lines, indicating the presence of basin outflow winds discussed by Whiteman et al. (1991); this does not appear to be a persistent, regularly occurring feature, however;
- Channeling of the airflows along the Kaibab Plateau is indicated in the 300 m AGL streak lines; and
- Transport to the south under northerly flows is indicated in both the 300 and 600 m AGL analyses.

Figure 9 is a time series plot showing when emissions from the NGS were probably present at the Grand Canyon and the associated category. Surface data collected at Hopi Point (winds, b_{sp}, direct solar radiation, temperature, relative humidity, and precipitation) and 700-mb heights measured at Tusayan also are shown. The results given in Fig. 9 indicate that periods of poor visibility, that is, values of b_{sp} greater than about 10–15 Mm^{-1}, coincide with the passage of synoptic-scale troughs through the study area, accompanied by southwesterly winds (note that light scattering by air alone is 10 Mm^{-1}). As reported in Richards et al. (1991), the occasions of worst visibility (i.e., highest b_{sp}) at Hopi Point (e.g., 20 January, 13 February, and 5 March) were associated with traveling storm systems and/or transport from the southwest or west accompanied by relative humidities greater than 70%. Of the worst 20% of re-

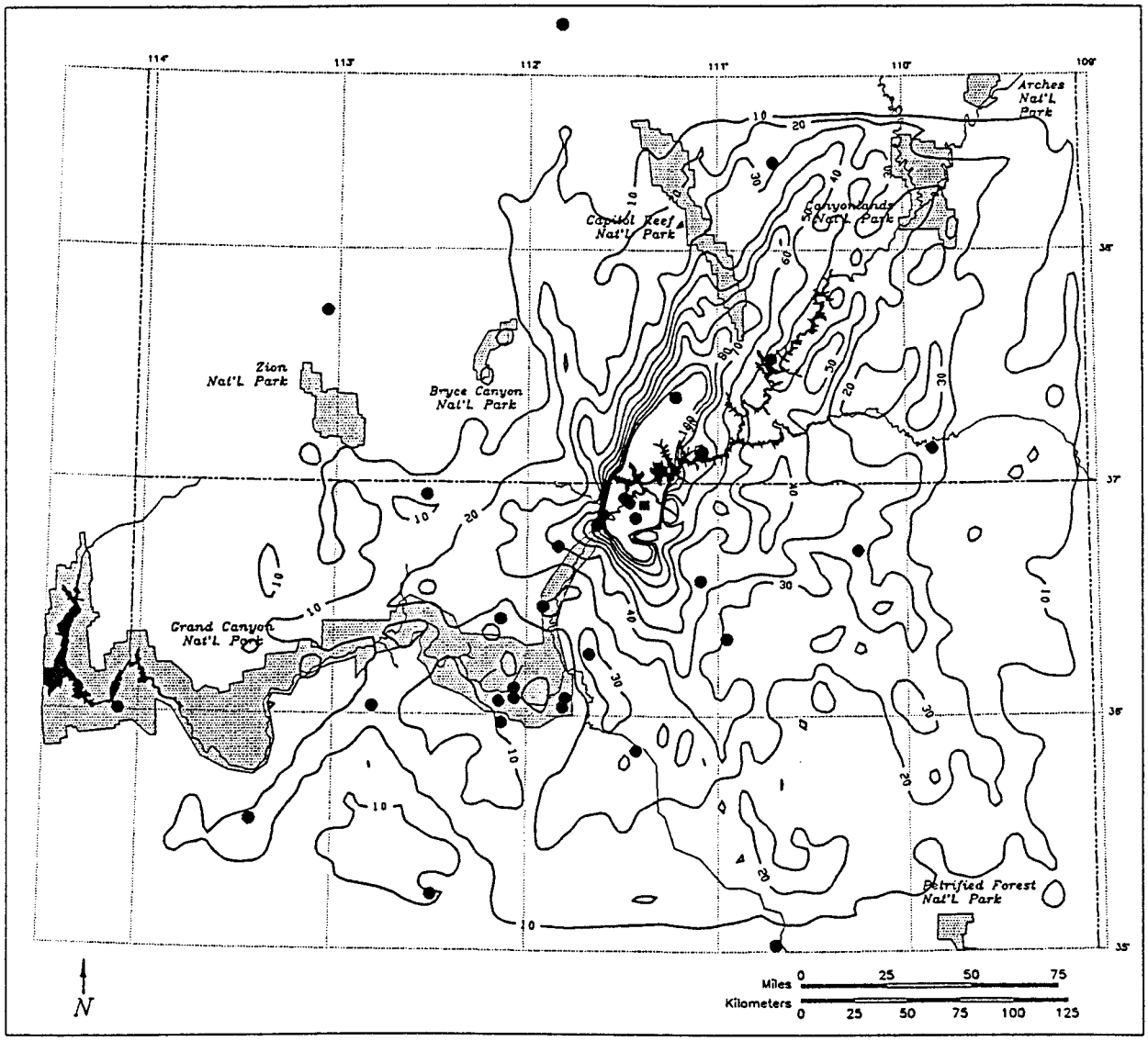

FIG. 8. Same as Fig. 7, for the 600 m AGL streak lines.

duced visibility episodes that occurred at GCNP during the study, all but one was associated with the passage of a synoptic-scale low pressure system. The results shown in Fig. 9 indicate that, with the exception of the 20 January and 31 March episodes, b_{sp} values greater than approximately 10–15 Mm^{-1} do not appear to coincide with the presence of NGS emittants at the Grand Canyon.

As indicated in Fig. 9, there were eight periods when NGS emittants were probably present at the Grand Canyon between 10 January 1990 and 31 March 1990. With one exception (February 28), the primary transport mechanism responsible for the initial transport of NGS emittants to the Grand Canyon was northerly-to-northeasterly winds that accompanied the passage of a synoptic-scale low pressure system through the study area, followed by the formation of a ridge of high pressure over the region. These flows were sometimes channeled by the major terrain features between Page and the Grand Canyon, especially the Kaibab Plateau. In most cases, the air mass carrying NGS emittants to the Grand Canyon was colder and dryer than the air mass that preceded the trough passage. In some cases, however, cloudiness and precipitation were still occurring and the plume may have mixed with the clouds before it reached the Grand Canyon. On a few occasions, a ridge of high pressure formed after the trough passage and persisted for several days, and a circulation formed over the region that carried NGS emittants in a clockwise manner through the study area. The cause of these circulations

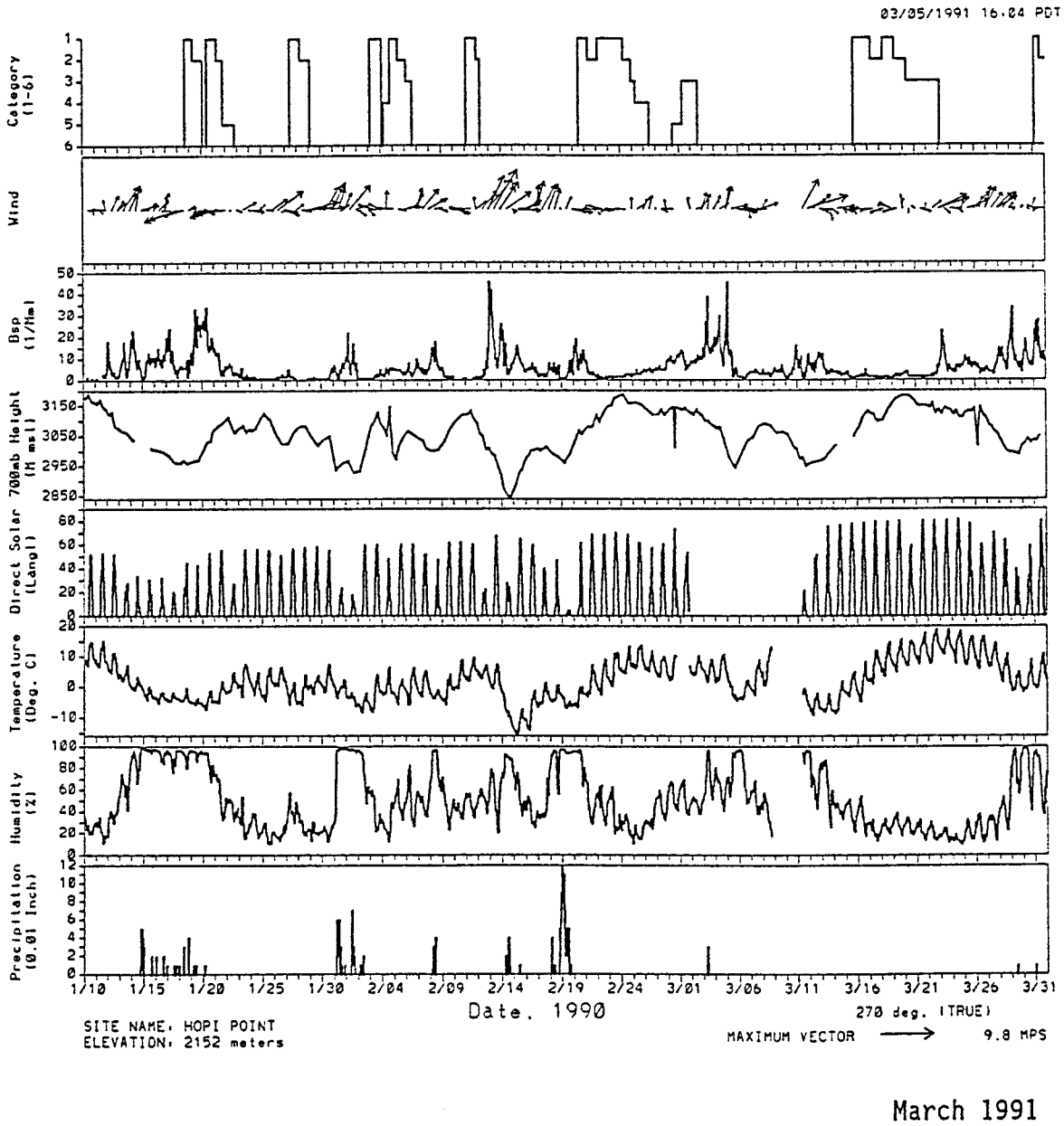

FIG. 9. Time series of surface winds, b_{sp}, direct solar radiation, temperature, relative humidity, and precipitation at Hopi Point; 700 mb heights at Tusayan; and the categories assigned when NGS emittants were probably present at the Grand Canyon for 10 January 1990–31 March 1990.

is still not clear, but they appear to be a response to the synoptic pressure gradient over the desert Southwest.

5. Case study: 18–22 January 1990

As indicated in Fig. 9, emissions from the NGS were believed to be at GCNP during eight periods of the field study. This section describes the meteorological processes responsible for the transport of these emissions during one of these periods, when emissions from the NGS may have contributed to visibility impairment in the GCNP. The results reported below are based on analyses of the transport patterns revealed by the computer animation and isentropic analyses described in the preceding sections, and on interpretation of surface and upper-air weather charts depicting synoptic-scale weather patterns during the period in question.

A synoptic-scale closed low pressure system passed through the study area on 18–19 January 1990. High humidities, clouds, and precipitation accompanied the passage of this storm system. Winds ahead of the low became easterly in the cyclonic circulation around the

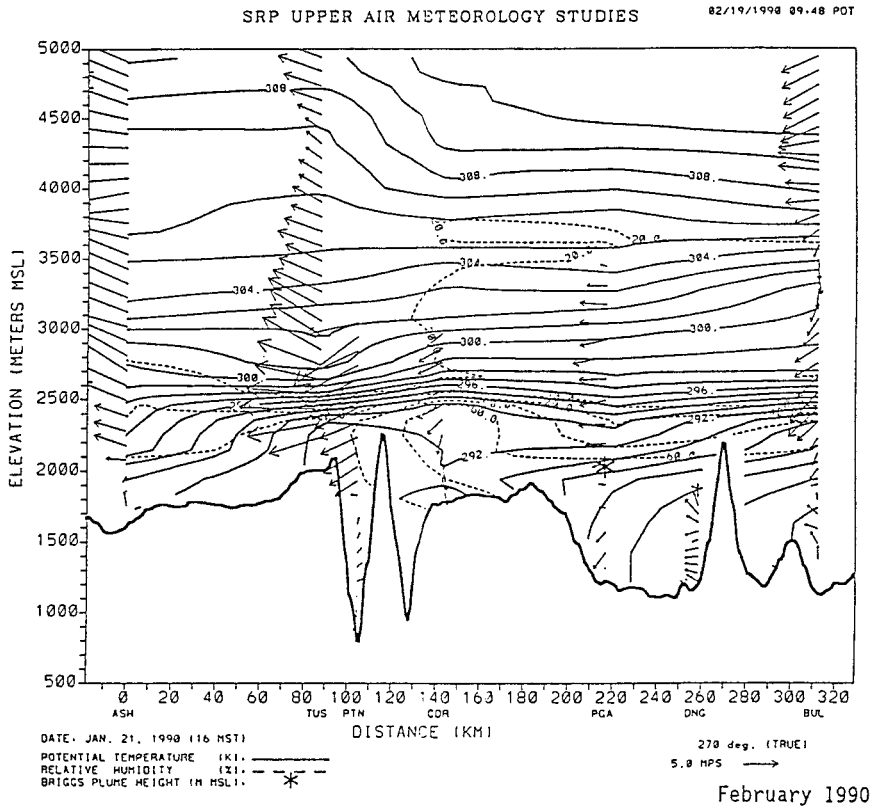

FIG. 10. Isentropic cross section for 1600 MST 21 January 1990. Solid lines are isentropes, dashed lines are isopleths of constant relative humidity, and vectors indicate wind speed and direction (north to top of figure, east to right of figure). The heavy solid line represents terrain elevations along the ground path of the cross section. Briggs plume height estimate of the altitude of the NGS plume is indicated by a star above Page.

northern side of the low. These easterly winds transported the NGS plume to the west and out of the study area. As the low swept through the study area, the winds reversed direction, backing to northerly and westerly, carrying emittants that were to the northwest and west of the Grand Canyon down across the park and out to the east. There was some evidence in the tracer data that emittants that had been carried out of the study area returned to the park in the westerly winds on 19 January.

For the 0200 and 0600 MST sampling periods on 20 January, NGS emissions were judged to be absent from the park as the westerly winds carried emittants to the east of the study area. The winds reversed direction again later on 20 January, becoming northerly and continuing to veer to easterly, as the 850-mb low moved out to the east and a ridge of high pressure formed at 850 mb over the study area. The 500-mb trough axis still extended through the study area, accompanied by northerly gradient winds. High relative humidities, cloudiness, and precipitation accompanied the passage of the low through the study area. As shown in Fig. 5, winds at plume height above Page were northeasterly (toward GCNP), and the relative humidity was high (70%–90%) at plume height. When the plume from the NGS reversed direction on 20 January as the low ejected out to the east and the ridge of high pressure formed, the plume was carried directly from Page over the park when the winds at plume height became northeasterly, and to Fredonia as the winds continued to veer to easterly. The 300 m AGL streak lines indicated that the winds in the lower part of the ABL were diverted and channeled by the Kaibab Plateau along the Marble Canyon Plain and on to the Grand Canyon. As a result, a portion of the NGS plume was carried directly to the west late on 20 January and early on 21 January, while another portion was carried toward GCNP.

By 21 January, a ridge of high pressure had built over northern Arizona. Subsiding dry air caused a strong inversion to form over the region. Figure 10 shows the isentropic cross section for 21 January at 1600 MST. The inversion extended over the Lake Powell basin and continued over the high terrain south of the Grand Canyon. The air in the basin was weakly stable. The Briggs plume-height estimate shows that the plume was in a moderately stable layer at an altitude below the high terrain along the Kaibab Plateau. Winds at plume height above Page were easterly. Note that the winds above the Marble Canyon plain at Cedar Ridge were decoupled

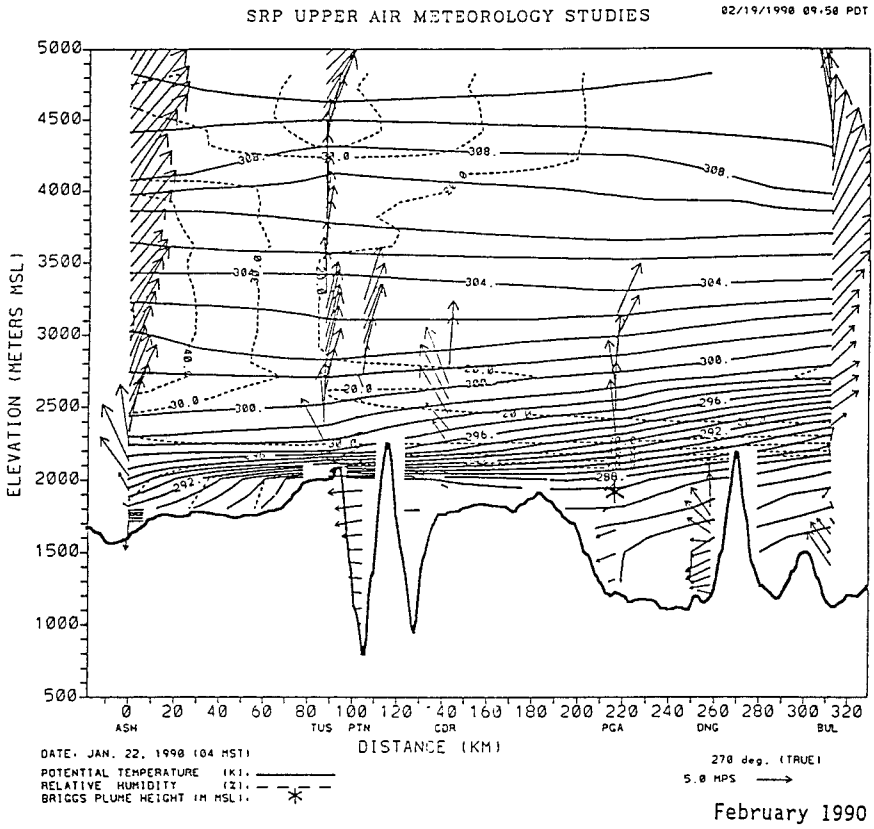

FIG. 11. Same as Fig. 10, except for 0400 MST 22 January 1990.

from the easterly winds within and above the inversion. The northerly winds of 3–4 m s^{-1} below the top of the terrain indicate that the flows in this layer were still being channeled along the Marble Canyon plain, and therefore these winds continued to transport NGS emissions along the Marble Canyon plain toward the Grand Canyon (see Fig. 3). This layer of northerly winds extended from the surface to approximately 450 m AGL. Above this altitude, the flows were from the southeast; the northerly winds in the lower layer persisted until approximately 0100 MST on 22 January. Winds in the Grand Canyon were generally upstream (westerly) on the afternoon of 21 January; however, in the upper part of the canyon, the winds were coupled with the synoptic-scale easterly flows aloft.

Figure 11 shows the conditions that existed at 0400 MST on 22 January. The inversion had descended over the region, effectively decoupling the winds in the Lake Powell basin and in the Grand Canyon from the synoptic-scale winds above the inversion. The Briggs plume-height estimate shows that the plume was trapped in the Lake Powell basin below the strong inversion. Above 2000 m MSL, temperatures were warmer over the high terrain south of the Grand Canyon than over the basin. This temperature gradient would suggest that air was flowing out of the basins. Indeed, winds at Dangling Rope and Page were easterly, indicating basin outflow toward the Fredonia Pass. However, winds along the Marble Canyon plain were southerly on January 22, whereas winds in the Grand Canyon were easterly through the depth of the canyon. This would indicate that the fresh plume was not being transported along the Marble Canyon plain to the Grand Canyon. Tracer and SO_2 data on the evening of 21 January and morning and early afternoon of 22 January indicated that NGS emittants were probably present at the Grand Canyon. These emittants were apparently transported along the Marble Canyon on 21 January and into the Grand Canyon on 22 January.

Richards et al. (1991) reported that the largest contributions to light scattering by particles at the Grand Canyon attributed to emissions from the NGS occurred during this episode and on 31 March. During the 18–22 January 1990 episode, b_{sp} measured at Hopi Point exceeded 10 Mm^{-1} from the 0200 MST sample on 19 January through the 0600 MST sample on 21 January (recall that light scattering by air alone is 10 Mm^{-1}). The maximum b_{sp} recorded during this episode was 29.98 Mm^{-1}, which occurred at 0600 MST on 20 January. However, the contribution of NGS emissions to light scattering during this sample was estimated to be only 1.2%. Richards et al. (1991) concluded that the largest contribution by NGS emissions to light scattering during this episode was 26%, which occurred in the

1400–1800 MST sample on 19 January, when the measured b_{sp} at Hopi Point was 23.4 Mm^{-1}. Conversion of SO_2 to sulfate can occur much more rapidly in cloud than in clear air. Since clouds and high humidities were present at GCNP during this period, it is likely that NGS SO_2 emissions that were transported to the park were mixed in cloud and converted to sulfate along the way, thus contributing to visibility reduction at the Grand Canyon.

6. Summary and conclusions

The 1990 NGS Visibility Study collected a rich meteorological database that has been used by investigators to examine meteorological processes affecting the transport of emissions from the Navajo Generating Station and the conditions that accompany visibility impairment at the Grand Canyon. The results of the analyses of the meteorological data reported here and by other authors lead to the following conceptual model of the mechanisms that can transport emittants from NGS to the Grand Canyon during the winter.

- Winds accompanying the passage of traveling storms are the primary mechanism responsible for transporting NGS emissions to GCNP. These winds are driven by the synoptic pressure gradient, and transport at plume altitudes is reasonably well coupled with flows through the middle and upper layers of the basins in the region.
- Mesoscale circulations form within the topography under clear, light wind conditions and can under some circumstances cause emissions from the NGS to be transported to the Grand Canyon.
- Slope and valley flows driven by the diurnal heating cycle can develop in the region during the wintertime, especially in the shallow surface layer. While such flows do not usually occur during active winter synoptic periods, they do appear under conditions of light winds aloft and clear skies, which are periodically interrupted by the passage of winter storms. NGS emittants mixed into the surface layer can be transported by these flows up or down slopes and along the axes of the major basins in the region. However, winds in these flows are generally light, typically less than 1–2 m s^{-1}, so that transport distances are relatively small. Traveling storms pass through the region often enough that taken as a whole, these slope and valley winds do not appear to be a significant mechanism for transporting emissions from the NGS to the Grand Canyon.

Mesoscale circulations are observed in the Lake Powell basin and inside the Grand Canyon itself, but these flows do not appear to be well coupled to each other. The Lake Powell basin outflows are typically east–west currents that carry NGS emittants in the middle part of the boundary layer (200–700 m AGL) toward Fredonia or up Lake Powell. Flows along the Marble Canyon plain do not regularly show that these basin outflows are channeled by the Kaibab Plateau toward the Grand Canyon or otherwise coupled with the outflows from the basin or from the Grand Canyon. The Grand Canyon currents typically are also east–west flows, but they do not appear to extend significantly past the eastern end of the Canyon below Desert View.

Synoptic-scale winds, channeled by the major terrain features of the regions, are the most important mechanism for transporting NGS emittants to the Grand Canyon. In the majority of cases when the plume is detected at GCNP, these winds accompany the passage of a trough of low pressure through northern Arizona. Emittants from NGS usually arrive at the Grand Canyon with the northerly winds that follow the passage of a low and the formation of a ridge of high pressure. Peak b_{sp} readings at the Grand Canyon, based on data collected at Hopi Point, also coincide with the passage of low pressure troughs. However, peak b_{sp} values usually occur in the prefrontal, southwesterly winds that occur before the trough sweeps through the region. Transport distances for the air masses arriving from the south or southwest with these storms are usually quite large, so that upwind, urban areas must be considered an important source region for these pollution events and poor visibility at the Grand Canyon.

Acknowledgments. Many people participated in the collection, processing, and analyses of the meteorological data collected during the NGS Winter Visibility Study. Dr. Rolland Hauser, California State University at Chico, was responsible for the collection and quality control of the surface data. Mr. William Knuth, Ms. Elaine Prins, Ms. Nancy Alexander, and Mr. Donald Lehrman assisted with the collection and review of the rawinsonde data. Dr. William Neff, Mr. Dan Wolfe, Dr. Robert Banta, and their colleagues at NOAA/ERL/ETL were responsible for operations of the radar profiler sites, the Phantom Ranch station, and the Doppler lidar. Dr. David Whiteman of Battelle Pacific Northwest Laboratories designed and performed the experiments at the Buffalo Ranch site, with assistance from Dr. Chris Doran. Mr. Kenneth Underwood and his colleagues from AeroVironment were responsible for the collection and review of the Doppler sodar data. We especially thank Mr. Jeff Prouty of STI for his hard work in the preparation of the computer animation. Finally, the first author would like to thank Drs. Hauser, Whiteman, Neff, Banta and his colleagues at STI for many discussions and insights that helped guide the research reported herein. This work was funded by the Salt River Project.

REFERENCES

Atkinson, B. W., 1981: *Mesoscale Atmospheric Circulations.* Academic Press, 495 pp.

Banta, R. M., L. S. Darby, P. Kaufmann, D. H. Levinson, and C.-J. Zhu, 1999: Wind-flow patterns in the Grand Canyon as revealed by Doppler lidar. *J. Appl. Meteor.*, **38,** 1069–1083.

——, and L. D. Olivier, 1991: Doppler lidar observations of air flow

in the Grand Canyon. Paper 91-47.11, *Proc. 84th Annual Meeting, Air & Waste Management Association*, Vancouver, BC, Canada, AWMA, 15 pp.

Briggs, G. A., 1972: Chimney plumes in neutral and stable surroundings. *Atmos. Environ.*, **6,** 507–510.

Chen, J., R. Bornstein, and C. G. Lindsey, 1999: Transport of a power plant tracer plume over Grand Canyon National Park. *J. Appl. Meteor.*, **38,** 1049–1068.

Goodin, W. R., G. M. McRae, and J. H. Seinfeld, 1980: An objective analysis technique for constructing three-dimensional urban-scale wind fields. *J. Appl. Meteor.*, **19,** 98–108.

Hauser, R. K., C. D. Whiteman, and J. L. Sutherland, 1991: Surface meteorological conditions during the winter 1990 Navajo Generating Station Visibility Impairment Study. Paper 91-47.9, *Proc. 84th Annual Meeting, Air & Waste Management Association*, Vancouver, BC, Canada, AWMA, 27 pp.

Lindsey, C. G., and D. E. Wolfe, 1991: Use of a new generation boundary layer profiler to investigate meteorological processes in complex terrain. Paper 91-57.8, *Proc. 84th Annual Meeting, Air & Waste Management Association*, Vancouver, BC, Canada, AWMA, 13 pp.

——, R. K. Hauser, W. E. Knuth, J. Chen, J. D. Prouty, and E. M. Prins, 1991: Meteorological measurements for the 1990 Navajo Generating Station Visibility Study. Final Rep. STI-99257-1171-FR, prepared for Salt River Project by Sonoma Technology, Inc., Santa Rosa, CA. [Available from Salt River Project, P. O. Box 52025, Phoenix, AZ 85072.]

——, T. S. Dye, and R. A. Baxter, 1995: Draft guidelines for the quality assurance and management of PAMS upper-air meteorological data. Final Rep. STI-94611-1556-FR, prepared for U.S. Environmental Protection Agency by Sonoma Technology, Inc., Santa Rosa, CA. [Available from U.S. Environmental Protection Agency, Office of Air Quality Planning and Structure, Research Triangle Park, NC 27711.]

Malm, W., K. Gebhart, D. Latimer, T. Cahill, R. Eldred, R. Pielke, R. Stocker, and J. Watson, 1989: National Park Service Report on the Winter Haze Intensive Tracer Experiment. Final Report.

National Research Council, 1990: Haze in the Grand Canyon: An evaluation of the winter haze intensive experiment. National Academy Press, Washington, DC. [Available from National Academy Press, 2101 Constitution Ave. NW, Washington, DC 20418.]

Orgill, M. M., 1981: Atmospheric studies in complex terrain: A planning guide for future studies, PNL-3656/ASCOT-80-4, Pacific Northwest Laboratory, Richland, WA.

Richards, L. W., and Coauthors, 1991: Navajo Generating Station Visibility Study Final Rep. STI-90200-1124-FR, prepared for Salt River Project by Sonoma Technology, Inc., Santa Rosa, CA.

Smith, T. B., 1981: Some observations of pollutant transport associated with elevated plumes. *Atmos. Eviron.*, **15,** 2197–2203.

Whiteman, C. D., 1990: Observations of thermally developed wind systems in mountainous terrain. *Atmospheric Processes Over Complex Terrain, Meteor. Monogr.*, No. 45, Amer. Meteor. Soc., 5–42.

——, K. J. Allwine, and J. M. Hubbe, 1991: Winter Meteorology of the Grand Canyon Region. Prepared for Salt River Project by Battelle Pacific Northwest Laboratories, Richland, WA, 292 pp. [Available from Salt River Project, P. O. Box 52025, Phoenix, AZ 85072.]

——, S. Zhong, and X. Bian, 1999a: Wintertime boundary layer structure in the Grand Canyon. *J. Appl. Meteor.*, **38,** 1084–1102.

——, X. Bian, and J. L. Sutherland, 1999b: Wintertime surface wind patterns in the Colorado River Valley. *J. Appl. Meteor.*, **38,** 1118–1130.